The Ninth Component of Complement and the Pore-Forming Protein (Perforin 1) from Cytotoxic T Cells: Structural, Immunological, and Functional Similarities

JOHN DING-E YOUNG, ZANVIL A. COHN, ECKHARD R. PODACK

The ninth component of complement (C9) and the pore-forming protein (PFP or perforin) from cytotoxic T lymphocytes polymerize to tubular lesions having an internal diameter of 100 Å and 160 Å, respectively, when bound to lipid bilayers. Polymerized C9, assembled by slow spontaneous or rapid Zn^{2+}-induced polymerization, and polyperforin, which is assembled only in the presence of Ca^{2+}, constitute large aqueous pores that are stable, nonselective for solutes, and insensitive to changes of membrane potential. Monospecific polyclonal antibodies to purified C9 and PFP show cross-reactivity, suggesting structural homology between the two molecules. The structural and functional homologies between these two killer molecules imply an active role for pore formation during cell lysis.

THE ASSEMBLY OF FUNCTIONAL PORES IN TARGET MEMbranes has long been viewed as an efficient way of mediating cell lysis (*1*). Membrane pore formation has been observed mainly in bacterial proteins, toxins, and antibiotics (*1*). Another role for pore formation in cell-mediated cytotoxicity has recently been proposed for the protozoan parasite *Entamoeba histolytica* (*2*), cytotoxic T and NK cells (*3, 4*), and eosinophils (*5*). One test for pore formation as a mechanism of cytotoxicity is the ability of pore-forming proteins purified from these cells of damaging directly target membranes, bypassing the need for intact cells. Pore-forming proteins (PFP's, named perforin 1, or P1) with such function were recently isolated from the cytoplasmic granules of cytotoxic T and NK-like lymphocytes (*6–8*). Perforin produces structural and functional membrane lesions (*6–8*) similar to those caused by intact cells and isolated granules (*9–13*).

A second immunological effector system that mediates killing by means of pore formation involves the membrane attack complex (MAC) of the complement cascade. This complex consists of a supramolecular assembly of the five terminal components of complement (C5b, C6, C7, C8, and C9) which produce cytolysis when inserted into target cell membranes to form tubular lesions (*14–16*), consistent with the transmembrane doughnut model for cytolysis proposed by Mayer *et al.* (*17*). The C9 component is the protein largely responsible for the formation of the ultrastructural membrane lesion associated with the MAC (*18, 19*), and purified C9 polymerizes into tubular complexes resembling the MAC (*19, 20*).

Although polymerized C9 (poly C9) has been shown to form structural membrane lesions, information on poly C9 as a functional transmembrane entity has not been available, especially since spontaneous polymerization of monomeric C9 is a slow process, requiring many hours of incubation at temperatures of or exceeding 37°C (*19, 20*). Reducing the time required for C9 polymerization severalfold and using isolated and homogeneous poly C9 has made it possible to resolve and dissect its molecular sieving properties in the membrane. Moreover, the possibility of functional and structural similarities between purified C9 and cytotoxic T cell perforin may now be addressed in a rigorous manner.

Zn^{2+} enhances C9 polymerization to functional channels. Spontaneous polymerization of C9 requires prolonged incubation of C9 at 37°C (*19, 20*), at a rate that would be too slow to be measured by standard cytotoxicity assays or electrophysiological measurements. Simultaneous C9 polymerization and channel formation need to be demonstrated but would only be likely to be observed if the time required for poly C9 formation were drastically reduced.

Zn^{2+} ions have been shown to inhibit C9-mediated hemolysis (*21*), possibly by enhancing C9 polymerization and consumption (*22*). As shown in Fig. 1, Zn^{2+} enhances the rate of C9 binding to lipid vesicles as demonstrated by isopycnic centrifugation (Fig. 1, E and F) compared to spontaneous association of C9 with lipid (Fig. 1, C and D). Zn^{2+} induces changes in the circular dichroism spectra of monomeric C9 similar to those observed during spontaneous C9 polymerization (*20*), indicating that Zn^{2+} may cause conformation changes in C9 with exposure of lipophilic domains. The enhanced polymerization of C9 by Zn^{2+} was further ascertained by ultrastructural analysis (Fig. 2). Poly C9 tubules in solution (Fig. 2, A and B) and in vesicle membranes (Fig. 2, C and D) formed by exposure to Zn^{2+} for 2 hours at 37°C were visualized by negative staining. In addition to tubular rings, a number of incomplete rings and linear polymers were also visualized. This material was used as a source for functional channel studies as follows. It was boiled in sodium dodecyl sulfate (SDS) and passed through a sucrose density gradient. This treatment allowed for enrichment of circular rings separating them from linear poly C9 (Fig. 2B). The rings were then used as a source of homogeneous material for single channel studies. On

J. D.-E Young and Z. A. Cohn are in the Laboratory of Cellular Physiology and Immunology, Rockefeller University, New York, NY 10021. E. R. Podack is in the Department of Microbiology and Immunology, New York Medical College, Valhalla, NY 10595.

SDS–polyacrylamide gel electrophoresis (PAGE), migration of SDS-resistant poly C9 indicated a molecular size of $>10^6$ daltons (Fig. 1G, lane 3), in contrast to the unfractionated material shown in Fig. 2A, which only showed partial resistance to dissociation by SDS under reducing conditions (Fig. 1G, lane 2).

Reconstitution of poly C9 channels into high resistance bilayers. The high impedance of planar lipid bilayers makes it possible to distinguish small current fluctuations with improved time resolution (*23*). Moreover, the planar bilayer system allows complete experimental control of the lipid, buffer, and voltage conditions, exposing C9 to a rigorous test of its ability to form channels. Exposing bilayers to monomeric C9 alone had no effect on bilayer conductance (Fig. 3A). However, incorporation of vesicles containing poly C9 into planar bilayers resulted in a current increase, which occurred in discrete steps (Fig. 3, A and B) and is consistent with the insertion of individual or groups of channels into the bilayer. The current increments were heterogeneous in size, which could be attributed to the heterogeneity of the poly C9 preparation used (legend to Fig. 3).

As noted above, the C9 channels were formed prior to their incorporation into planar bilayers (Fig. 3, A and B). The Zn^{2+}-induced polymerization of C9 with simultaneous functional channel formation could also be demonstrated. Addition of Zn^{2+} and monomeric C9 to a bilayer at 37°C resulted in a rapid rise of membrane conductance (Fig. 3D). The increase in conductance could be slowed considerably by decreasing the temperature to 30°C, and under these conditions formation of individual channels was resolved (Fig. 3E). Insertion of large conductance steps into planar bilayers is also an attribute of the pore-forming protein (perforin 1) isolated from cytotoxic T lymphocytes and NK-like lymphocytes. However, unlike C9, the lymphocyte perforin inserts spontaneously into bilayers at room temperature (22° to 24°C) and only in the presence of Ca^{2+} (*8*). Moreover, the Ca^{2+} requirement for perforin-mediated hemolysis cannot be substituted by Zn^{2+} or Mg^{2+} (*7*).

Voltage dependence, single channel fluctuations, ion selectivity, and pore size. Poly C9 channels could not sense voltage polarity in that the transmembrane current flow through these channels was symmetrical regardless of the sign of the voltage applied (Fig. 3C). Poly C9 channels were also resistant to an increase in electrical field, the current driven through these channels showing little or no relaxation to lower steady-state values up to a transmembrane potential of 110 mV (Fig. 4A). This point could be further illustrated by the continuous current-voltage (I-V) plot generated by passing a voltage ramp from −240 to +240 mV (Fig. 4B), an indication that the current tracing remains linear (that is, ohmic) until voltages higher than 100 mV are reached. At more than 100 mV, the current trace becomes "noisy" and shifts from linearity, suggesting closing of individual poly C9 channels at high voltages. Thus, poly C9 forms stable, voltage-insensitive channels that remain open in the physiological range of membrane potential and thus resemble the perforin channels of cytotoxic lymphocytes (*8, 11*), an observation that would be consistent with the cytolytic function attributed to MAC and polyperforin.

Single poly C9 channel fluctuations were obtained by lowering the amount of poly C9 incorporated into the bilayer and by

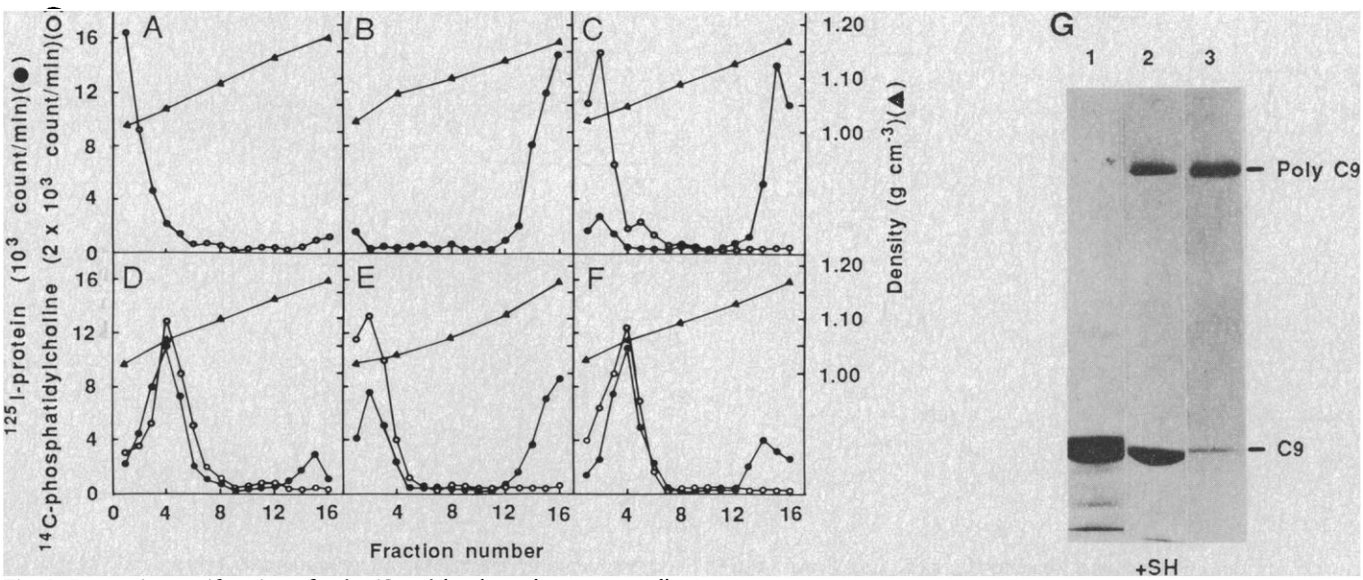

Fig. 1. Isopycnic centrifugation of poly C9 vesicles through sucrose gradients. Vesicles (A–E) were prepared from egg phosphatidylcholine and cholesterol (*37*). C9, purified from human plasma (*16, 19*), was incubated with vesicles in buffer A at a ratio of protein to lipid of 1:5 (by weight) at 37°C for the following lengths of time: (C) 2 hours; (D) 64 hours; (E) in the presence of 1 m*M* $ZnCl_2$ for 30 minutes; (F) with 1 m*M* $ZnCl_2$ for 2 hours. Portions of C9 vesicles (10 μg of C9 in 0.5 ml of 40 percent sucrose (w/v) were transferred to cellulose nitrate tubes, overlaid with 5 ml of a continuous sucrose gradient (5 to 35 percent) and centrifuged for 16 hours at 190,000*g* at 4°C in a SW50 rotor. Fractions of 0.25 ml were collected and numbered from top. Total radioactivity per fraction is given. C9 was labeled with ^{125}I to 1100 count/min per nanogram and was used at an input of 4×10^4 count/min per tube as a marker for protein (●). [*Choline methyl*-^{14}C]phosphatidylcholine (8×10^4 count/min) was used as a marker for lipid (○). Sucrose density was determined by refractometry (▲). In (A), vesicles were centrifuged in the absence of protein; vesicles floated to the top. (B) C9, in the absence of lipid, was found in the bottom. Note that after 2 hours of incubation (C), very little C9 comigrated with lipid. Lipid association was essentially complete after 64 hours (D). In contrast, Zn^{2+} caused virtually complete association of C9 with lipid after 2 hours (F). (G) SDS–polyacrylamide gel electrophoresis profile of monomeric and polymeric C9. (Lane 1) Monomeric C9; (lane 2) poly C9; C9 at 1 to 3.5 mg/ml in 0.15*M* NaCl, 10 m*M* tris-HCl, 1 m*M* $ZnCl_2$, 3 m*M* NaN_3, 2 m*M* phenylmethanesulfonyl fluoride, and soybean trypsin inhibitor at 50 μg/ml, *p*H 7.2 (TBS) was incubated for 2 hours at 37°C. (Lane 3) Poly C9 isolated by rate zonal centrifugation. Poly C9 (used for lane 2), was first incubated with 2 percent SDS and boiled for 2 minutes when 10 percent deoxycholate was added. The material was separated on a Sepharose C1-4B column with subsequent centrifugation, on a sucrose density gradient (5 to 20 percent) (*19*). The 27*S* pool was used in lane 3. This treatment was enriched for circular polymers, which showed resistance to dissociation by SDS, in contrast to the unfractionated poly C9 pool (lane 2). The electrophoresis was conducted under reducing conditions (*19*); 5 μg of protein was applied to each lane.

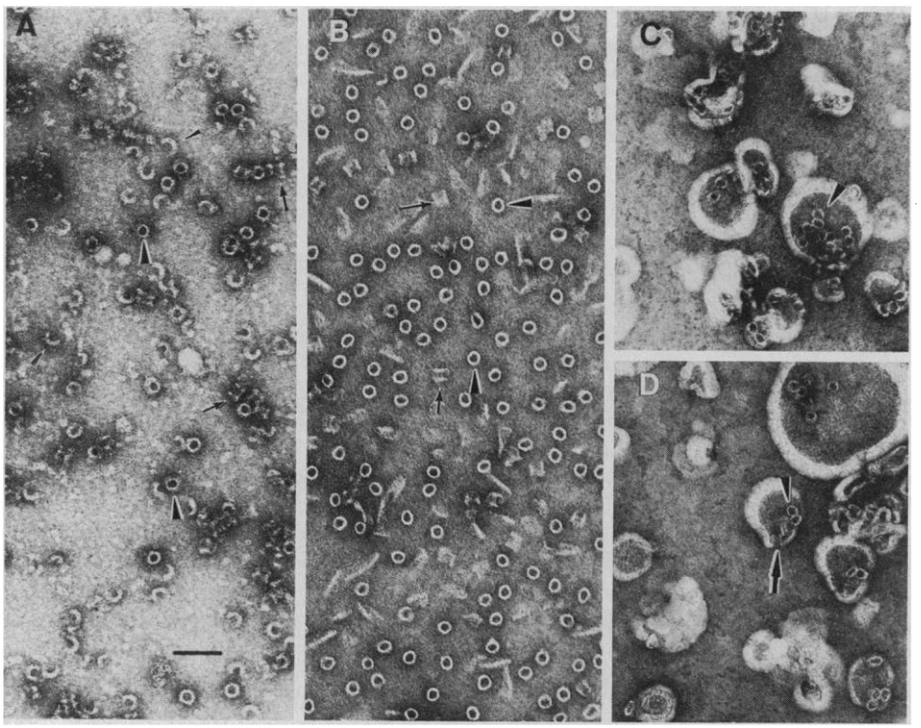

Fig. 2. Ultrastructure of poly C9 lesions assembled in the presence of $ZnCl_2$. Samples were negatively stained with 2 percent uranyl formate. (A) Poly C9: same material as that used for Fig. 1G, lane 2. Ring structures in side views (arrows) and top view projections (large arrowheads) are shown. Linear noncircular poly C9 are depicted by small arrowheads. (B) Circular poly C9: material used for Fig. 1G, lane 3. Typical ring structures are seen in side view (arrows) and top view (arrowheads) projections. This population of homogeneous circular complexes was used for single channel sizing (Fig. 5E). (C and D) Selected images of poly C9 lesions assembled on lipid vesicles. Poly C9 vesicle complexes were prepared by incubating the 27*S* tubular poly C9 pools described above with egg lecithin and removal of deoxycholate by dialysis. Side view (arrows) and top view (arrowheads) projections of tubular membrane lesions are shown (scale bar, 500 Å).

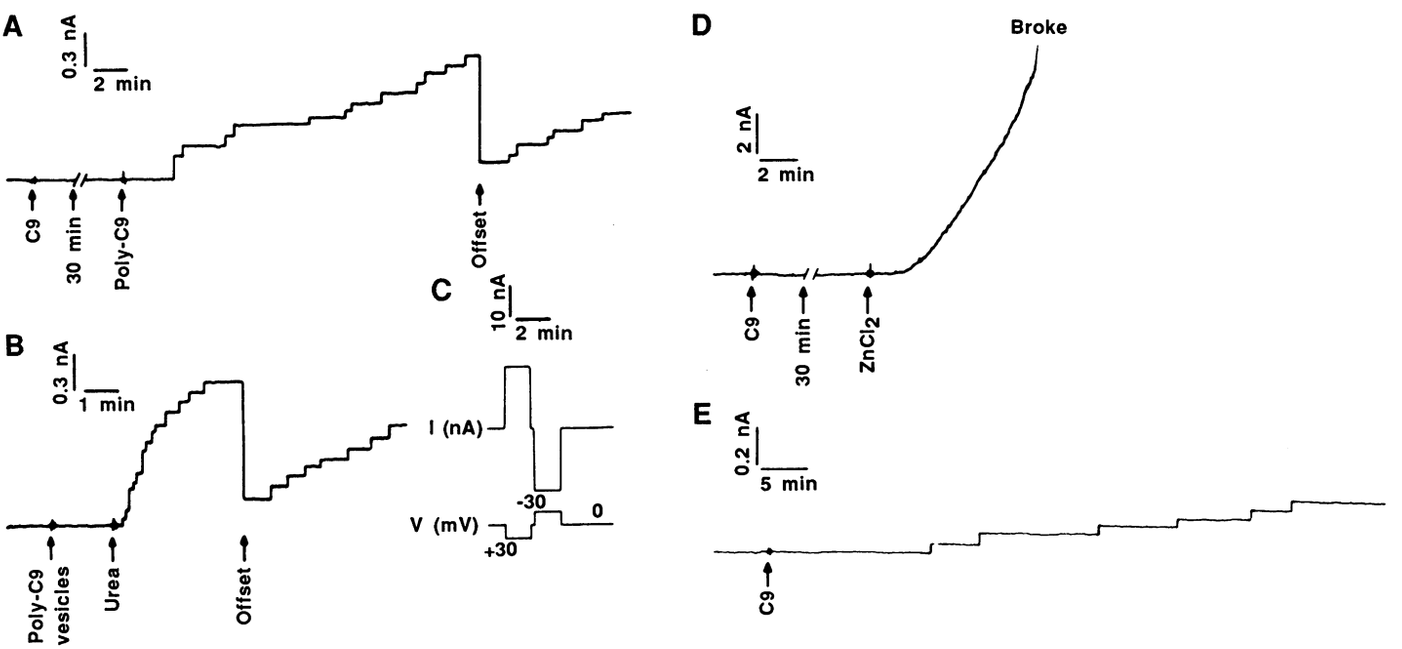

Fig. 3. Formation of functional channels by poly C9. Planar bilayer membranes (*23, 26*) showed a baseline conductance (*g*, expressed in siemens, 1 S = A/V) that did not exceed 10 pS. The bilayers were made from soybean phospholipids (*37*) in 0.1*M* NaCl, 1 m*M* $CaCl_2$, 5 m*M* Hepes, 3 m*M* NaN_3, *p*H 7 (buffer A) and clamped at a constant +30 mV throughout the experiments, positive current being defined as flowing from *cis* to *trans*. All reagents were introduced in volumes that did not exceed 0.25 percent of the total volume of membrane buffer and to the *cis* side unless otherwise indicated. (A) C9 was applied to the aqueous phase to 15 μg/ml (arrow), with immediate stirring (noise). Monomeric C9 did not change bilayer conductance. Poly C9 (prepared as in Fig. 1G) dissolved in 0.1 percent Triton X-100, was added 34 minutes later, to 3.5 μg/ml (*38*). The current progressively increased in discrete steps, until the current trace was offset manually to allow continuous observation of the incorporation of the C9 channel. (B) Incorporation of poly C9 vesicles into the bilayer by a fusion protocol (*39*), in the absence of detergent. Vesicles were added to the bilayer prepared in buffer A containing 15 m*M* $CaCl_2$, and clamped at +30 mV. Urea was then added to the same side to 300 m*M*. The incorporation of current steps into the bilayer, demonstrates that incorporation of poly C9 channels could also be accomplished in the absence of any detergent. Poly C9 vesicles were prepared by a detergent dialysis protocol (*36*) with the use of egg lecithin and cholesterol (3*M*:1*M*) and C9 at a ratio of protein to lipid of 1:5 by weight. Dialysis was performed for 64 hours at 37°C. (C) Symmetry of poly C9–associated current in response to voltages of opposite polarities. The bilayer in (A) was left at 0 mV for 45 minutes before the application of two voltage pulses of +30 and −30 mV, as indicated in the lower trace (V). Experiments (A to C) were performed at 22° to 24°C. (D) Effect of Zn^{2+} on C9 polymerization and channel formation. C9 (200 μg/ml) was added to a bilayer formed in 0.1*M* NaCl, 1 m*M* $CaCl_2$ and 10 m*M* tris-Cl, *p*H 8 (buffer B) and clamped at +30 mV. The experiment was performed at 37°C. The trace interrupted with parallel bars indicates absence of current activity. $ZnCl_2$ was then added to 1 m*M*, and there was immediate current activity until the membrane broke. (E) C9 (25 μg/ml) was added to a bilayer prepared in buffer B containing 50 μ*M* $ZnCl_2$ at 30°C. The bilayer was clamped at +30 mV. The slow stepwise increments in current are in contrast to a much higher current activity observed at 37°C (D).

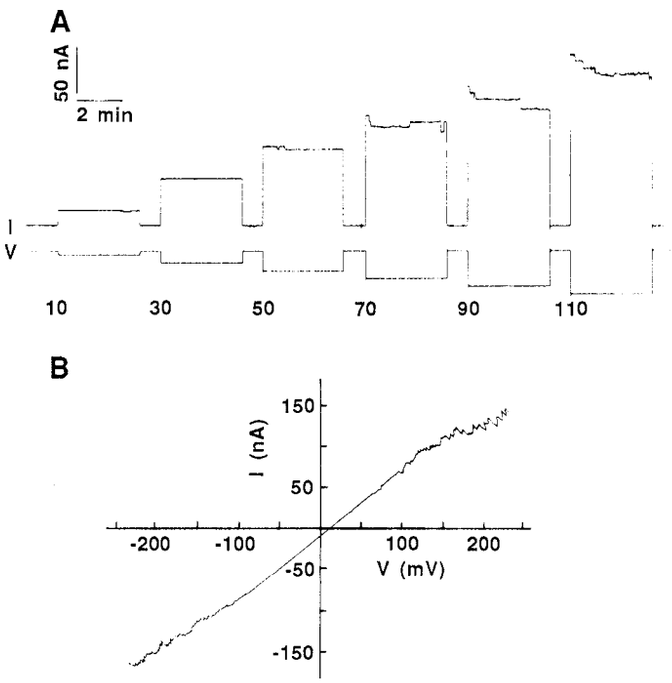

Fig. 4. Voltage-dependence of poly C9 channels. (A) A bilayer, in buffer A, was treated with poly C9 at 3.5 μg/ml as in Fig. 3A; 30 minutes later, voltage steps of 4-minute duration were applied (lower trace). The voltage was turned off for 1 minute between the two steps. The final current (after 4 minutes) was defined as the steady-state current, and it was used to generate current-voltage (I-V) plots [plots similar to that generated by a continuous voltage ramp (B)]. There is little relaxation of current in response to voltage increments up to +110 mV. Discrete current steps, corresponding to closing of individual poly C9 channels, were infrequently observed when the voltage exceeded +70 mV. (B) Continuous I-V relations obtained with a voltage ramp. The bilayer was prepared and treated with poly C9 as in (A). A continuous triangular pulse lasting 90 seconds was applied from −250 to +250 mV. The current obtained during the ramp was plotted as a function of the applied voltage. The current response from −100 to +100 mV is linear but deviated from linearity outside this range.

increasing the transmembrane potential to more than 120 mV (Fig. 5, A and B). Open channel lifetimes persisted from seconds to several minutes (Fig. 5, A and B). Several intermediate states with shorter lifetimes were also observed. The transmembrane current driven through each poly C9 channel increased linearly with an increase in the ionic strength of the bathing medium (Fig. 5C), an indication that water and ions are freely mobile within the poly C9 channel; this is consistent with a water-filled transmembrane tubular model for poly C9 channel.

Histograms of single poly C9 channel conductance showed a wide distribution of sizes (Fig. 5D), ranging from 0.2 to 4 nS (mean of 1.5 nS) per channel in 0.1*M* NaCl, *p*H 7.0. The scatter in the data probably reflects heterogeneity of the poly C9 population, as indicated by the substantial number of incomplete, half and double rings viewed by electron microscopy (Fig. 2A). This distribution was narrowed and the scatter in the data was reduced when a population of homogeneous SDS-resistant poly C9 (obtained by enrichment through centrifugation, as shown in Fig. 1G, lane 3, and Fig. 2B) was used for sampling, which resulted in a mean conductance of 2 nS per channel (Fig. 5E). Alternatively, a narrower single channel distribution was also collected when 0.5*M* Hepes-tris

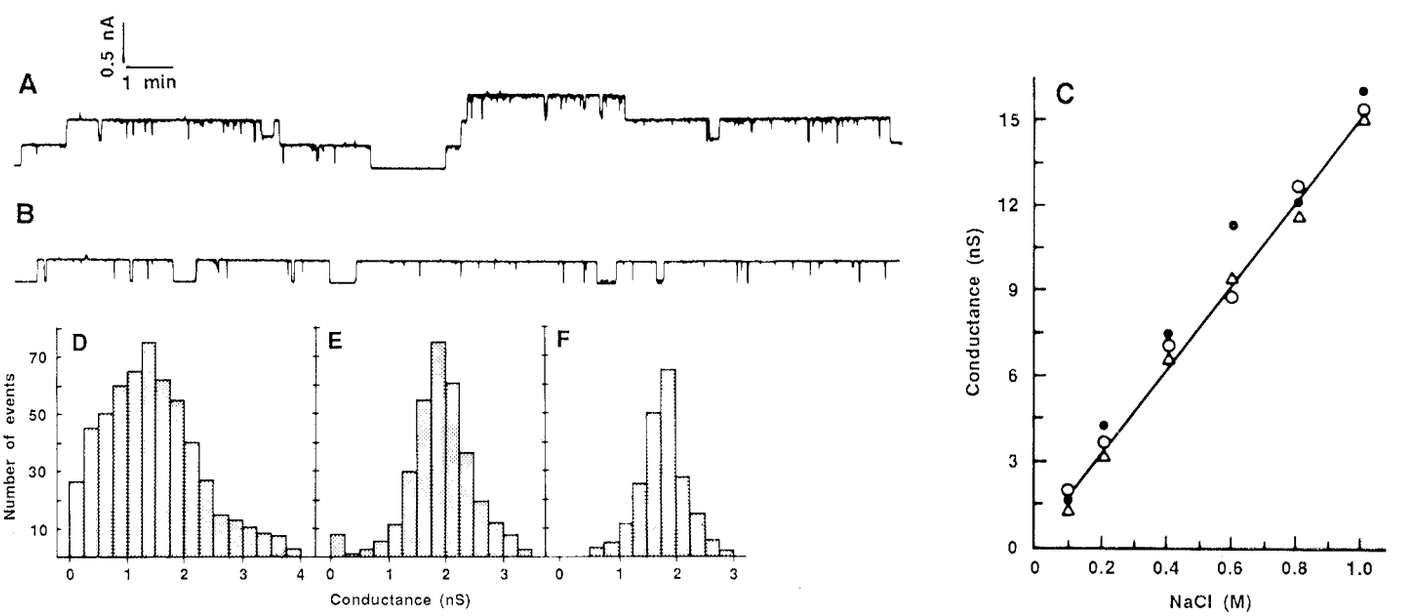

Fig. 5. Poly C9 single channel fluctuations. (A and B) Bilayers prepared in buffer A. A homogeneous preparation of circular poly C9, prepared as described in Fig. 1G, was mixed with 0.1 percent Triton X-100 and added (A) at 1.5 ng/ml and (B) at 0.7 ng/ml. The bilayers were clamped at +120 mV in both traces. Note single channel fluctuations and a few intermediate steps. (C) Single channel conductance as a function of the ionic strength of the membrane buffer. Data points represent three separate experiments. (●, ○) Two experiments performed with the same batch of homogeneous poly C9 obtained by rate and zonal centrifugation. (△) A different batch of poly C9. Bilayers were made in buffer A. Poly C9 (2 ng/ml) in 0.1 percent Triton X-100 was added. Single channel amplitude was obtained by applying pulses of +120 mV. The ionic strength of the buffer was changed by perfusion with ten volumes of membrane buffer essentially as described (*38*). (D to F) Histograms of frequency of single channel conductance. (D) Bilayers were prepared in buffer A. Poly C9 was prepared as in Fig. 3A. Single channel recordings used for sampling were obtained as in (C). (E) Use of circular poly C9 enriched by rate zonal centrifugation (Fig. 1G). Three different batches were used for sampling. (F) Bilayers bathed in 0.5*M* Hepes-tris, *p*H 7, were exposed to the same material used to generate the histogram in (D). Within the same group, different batches gave similar results. Thus, the broad distribution shown in (D) does not represent a summation of different distributions that could be attributed to variations between batches used. The scatter in the data seen in (D) is reduced when homogeneous material is used (E) and when larger electrolytes (Hepes, tris) are used for sieving.

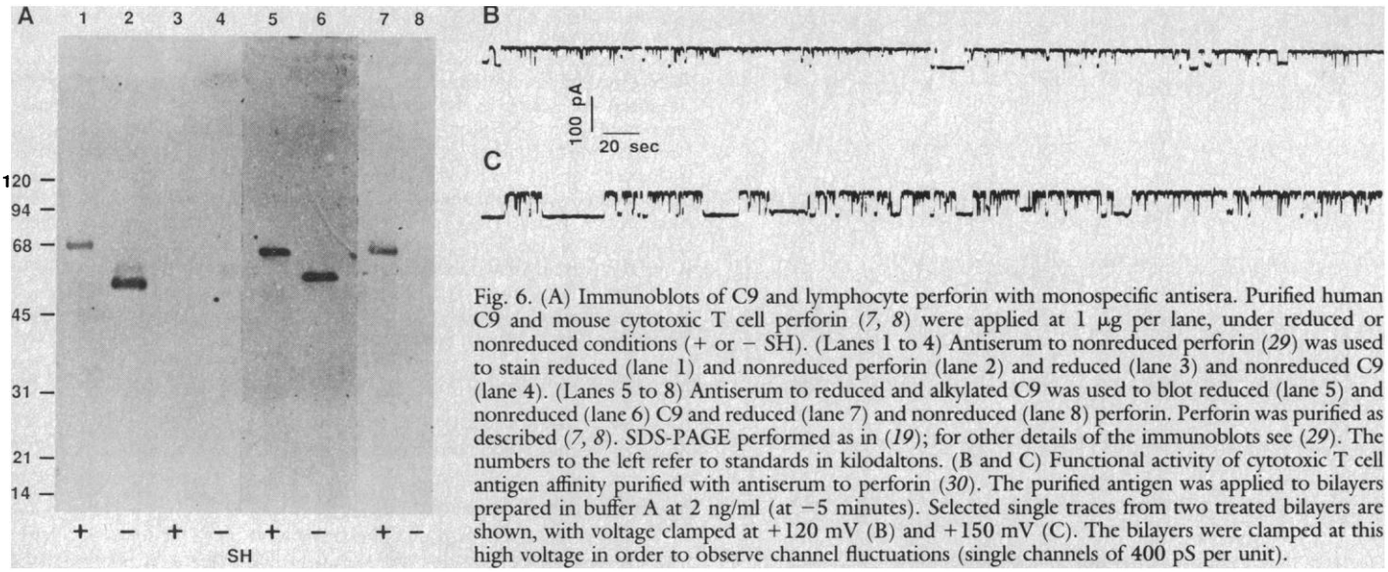

Fig. 6. (A) Immunoblots of C9 and lymphocyte perforin with monospecific antisera. Purified human C9 and mouse cytotoxic T cell perforin (*7, 8*) were applied at 1 μg per lane, under reduced or nonreduced conditions (+ or − SH). (Lanes 1 to 4) Antiserum to nonreduced perforin (*29*) was used to stain reduced (lane 1) and nonreduced perforin (lane 2) and reduced (lane 3) and nonreduced C9 (lane 4). (Lanes 5 to 8) Antiserum to reduced and alkylated C9 was used to blot reduced (lane 5) and nonreduced (lane 6) C9 and reduced (lane 7) and nonreduced (lane 8) perforin. Perforin was purified as described (*7, 8*). SDS-PAGE performed as in (*19*); for other details of the immunoblots see (*29*). The numbers to the left refer to standards in kilodaltons. (B and C) Functional activity of cytotoxic T cell antigen affinity purified with antiserum to perforin (*30*). The purified antigen was applied to bilayers prepared in buffer A at 2 ng/ml (at −5 minutes). Selected single traces from two treated bilayers are shown, with voltage clamped at +120 mV (B) and +150 mV (C). The bilayers were clamped at this high voltage in order to observe channel fluctuations (single channels of 400 pS per unit).

replaced electrolytes as the sieving species (Fig. 5F). This result could be due to the larger hydration radii of Hepes and tris so that only channels of larger size were selected.

A channel of the size described here (ranging from 0.2 to 4 nS in 0.1*M* NaCl) would be expected to allow an ion flow of at least 10^9 ions per channel per second. This rate is one to two orders of magnitude larger than that observed with a number of other constitutive membrane channels (*1*), but resembles that produced by the PFP of cytotoxic lymphocytes (*8, 11*). By modeling poly C9 channel as a tubular structure with interior specific conductance similar to that of the external solution (*24*), we obtain an estimated diameter of 60 to 80 Å for the poly C9 channel. These estimates are comparable to the minimal functional diameters of 40 Å (*25*) and 55 Å (*26*) estimated for the MAC.

As would be expected for a channel of this size, poly C9 shows little ion selectivity. Permselectivity ratios of 1.6:1.4:1:0.3 for K^+:Na^+:Cl^-:Ca^{2+} were obtained (*27*), indicating that poly C9 functions as a nonselective ion filter. These selectivity ratios are comparable to those of the entire MAC reconstituted into planar bilayers (*27*). Poly C9 also showed poor selectivity to Li^+, Mg^{2+}, Zn^{2+}, Mn^{2+}, Ba^{2+}, I^-, and Br^-.

Electrolyte and macromolecule sieving properties were also examined in lipid vesicles carrying polymerized C9, which allows studies of bulk transfer of solutes across membranes. Poly C9–bearing vesicles were leaky to markers like lucifer yellow (457 daltons) and sucrose (342 daltons) (*28*).

Immunological cross-reactivity between C9 and perforin. The resemblance in ultrastructural morphology and functional properties between C9 and perforin suggested the presence of structural domains common to both molecules. This possibility was assessed with the use of polyclonal antibodies to purified C9 and perforin (*29*). As is shown in Fig. 6A, immunostaining with a polyclonal antiserum to reduced and alkylated C9 (*29*) revealed activity with both reduced (lane 5) and nonreduced (lane 6) C9 and also reduced

Table 1. Similarities and differences between C9 and perforin.

Feature	C9	Perforin 1*
Molecular mass (SDS-PAGE)	70 to 75 kD (reduced) 62 to 66 kD (nonreduced)	70 to 75 kD (reduced) 60 to 64 kD (nonreduced)
Polymerization into tubules catalyzed by	C5b-C8, heavy metals (Zn^{2+} most effective), temperature >37°C	Ca^{2+}, temperature >30°C
Internal diameter of tubule by EM	100 Å	160 Å
Unit conductance step in 0.1*M* NaCl	0.2 to 4 nS	0.4 to 6 nS†
Electrical characteristics	Voltage-resistant, open state favored, slow channel kinetics	Voltage-resistant, open state favored, slow channel kinetics
Functional size	Permeable to monovalent and divalent ions, Lucifer yellow and sucrose	Permeable to monovalent and divalent ions, Lucifer yellow, sucrose, and glucosamine
Antigenic cross-reactivity	(+) Antiserum to reduced perforin (−) Antiserum to nonreduced perforin	(+) Antiserum to reduced C9 (−) Antiserum to nonreduced C9
Cytotoxicity	Hemolytic activity requires activation of C5b-C8; cytolytic to a variety of tumor cell lines	Hemolytic; cytolytic to a variety of tumor cell lines; cytolysis requires Ca^{2+}

*Perforin refers to material purified from mouse cytotoxic T cell lines and NK-like lymphocytes (*7, 8*). Similar results have been obtained with human large granular lymphocytes and NK-cell lines. C9 refers to human material described in the text. †This range of channel sizes includes data obtained on channels formed by perforin added directly to the aqueous phase of planar bilayers at room temperature (with unit conductances of 0.4 nS) and also by polyperforin polymerized in lipid vesicles at 37°C prior to incorporation into planar bilayers (which range 1 to 6 nS) (*8, 31*). The range of channel sizes for C9 shown here pertain only to poly C9 complexes previously formed and transferred to planar bilayers (as shown in Fig. 5).

perforin (lane 7); but there was no activity with native, nonreduced perforin (lane 8). The antiserum to nonreduced C9 (*29*) stained C9 but not perforin (see Table 1). Analogously, the antiserum to purified and reduced perforin (*29*) showed immunostaining with both forms of perforin and only reduced C9. Finally, antiserum to purified (native, nonreduced) perforin immunoblotted with both reduced (Fig. 6A, lane 1) and nonreduced (lane 2) perforin, as expected, but not C9 (reduced, lane 3; nonreduced, lane 4).

Affinity-purified antibodies isolated from antiserum to perforin (*30*) were used to separate perforin from cytotoxic T cell lysates by affinity chromatography (Fig. 6B). The purified and reduced protein migrated with an apparent molecular size of 70 to 75 kD on SDS-PAGE (with a profile similar to that shown in Fig. 6A). When added to planar bilayers, this protein inserted into membranes as nonspecific ion channels with large unit conductances and with a number of characteristics similar to C9 (Fig. 6, B and C), and (Table 1) (*31*). Taken together, these data imply a structural and functional homology shared by C9 and lymphocyte perforin. The shared domain is probably limited to a cysteine-rich domain that is immunologically exposed only when the protein is reduced. It should be pointed out that while the immunological cross-reactivity described here is based on results obtained with several polyclonal antibodies prepared against different forms of C9 and perforin, the extent of structural homology would be better assessed if monoclonal antibodies to C9 or perforin were used. Preparation of such monoclonal antibodies could result in delineating more accurately the cross-reactive domains.

We point out that the purified perforin lyses erythrocytes and tumor cells in the presence of Ca^{2+} (*8*) in contrast to C9, which requires the assembly of C5b-C8 in the target membrane before insertion into the bilayer and its subsequent polymerization to cause target cell lysis.

Conclusions. The association of antigen, antibody, and complement has been shown to result in increased membrane permeability (*32*). The permeability increase associated with the MAC was only observed when C8 and C9 were present (*33*). Single channel fluctuations have also been recorded in the presence of complement reaction associated with antigen-antibody complexes (*34*). However, little was known about the molecular nature or components of the membrane lesion since all previous published experiments involved multimolecular reactions. The demonstration here that one single protein species (C9) is capable of producing functional membrane lesions provides a direct correlation of structure and function of complement lesions.

In vivo, the activation of C5b-8 would be expected to anchor and accelerate C9 polymerization in the target membrane, resulting in the nucleation and localization of a circular membrane lesion. This view is consistent with the observation that under appropriate conditions (as in the presence of Zn^{2+} and higher temperatures), C9 polymerization may be accelerated manyfold. Alternatively, C5b-8 may also play a direct cytolytic role, with formation of functional channels at the C8 stage (*33*), which would be consistent with the observation that, in the absence of C9, complement-mediated cytolysis may still occur, albeit at a slower rate (*35*). The channels formed by C8, however, show totally different unitary conductances, channel kinetics and voltage-current relationships from those observed for poly C9 [see also footnote in (*34*)]. Finally, the number of C9 subunits required to produce a functional lesion is not known at present.

We have some data indicating that, as in the case of lymphocyte perforin (*8*), functional lesions may be produced by C9 prior to its complete polymerization into macromolecular tubular lesions (*36*).

It is intriguing that C9 and perforin should share a number of structural and functional similarities (Table 1). Both species form large aqueous channels with little ion selectivity and are relatively resistant to the effects of transmembrane electrical field. It is conceivable that such attributes may favor an active role of these proteins in cytolysis. Once inserted into target membranes, poly C9 and perforin channels would be expected to remain open, regardless of the cell membrane potential. The free permeation of ions, water, and macromolecules through such channels, resulting in disruption of transmembrane gradients, may all contribute to the lethal effect. Pore formation resulting in target membrane damage may represent a general mechanism of cytotoxicity. It is possible that at least some of these proteins may have emerged from the same ancestral protein during evolution but diverged and became specialized later to carry out either humoral or cellular immune responses.

REFERENCES AND NOTES

1. R. Latorre and O. Alvarez, *Physiol. Rev.* **61**, 77 (1981); S. J. Schein, B. L. Kagan, A. Finkelstein, *Nature (London)* **276**, 159 (1978).
2. E. C. Lynch, I. M. Rosenberg, C. Gitler, *EMBO J.* **1**, 801 (1982); J. D.-E Young, T. M. Young, L. P. Lu, J. C. Unkeless, Z. A. Cohn, *J. Exp. Med.* **156**, 1677 (1982); C. Gitler, E. Calef, I. Rosenberg, *Philos. Trans. R. Soc. London* **307**, 73 (1984); J. D.-E Young and Z. A. Cohn, *J. Cell. Biochem.* **29**, 299 (1985).
3. R. R. Dourmashkin, P. Deteix, C. B. Simone, P. A. Henkart, *Clin. Exp. Immunol.* **42**, 554 (1980).
4. G. Dennert and E. R. Podack, *J. Exp. Med.* **157**, 1483 (1983); E. R. Podack and G. Dennert, *Nature (London)* **302**, 442 (1983).
5. J. D.-E Young, C. G. B. Peterson, P. Venge, Z. A. Cohn, *Nature (London)* **321**, 613 (1986).
6. D. Masson and J. Tschopp, *J. Biol. Chem.* **260**, 9069 (1985).
7. E. R. Podack, J. D.-E Young, Z. A. Cohn, *Proc. Natl. Acad. Sci. U.S.A.* **82**, 8629 (1985).
8. J. D.-E Young, H. Hengartner, E. R. Podack, Z. A. Cohn, *Cell* **44**, 849 (1986); J. D.-E Young, E. R. Podack, Z. A. Cohn, *J. Exp. Med.* **164**, 144 (1986).
9. P. J. Millard, M. P. Henkart, C. W. Reynolds, P. A. Henkart, *J. Immunol.* **132**, 3197 (1984); R. Blumenthal, P. J. Millard, M. P. Henkart, C. W. Reynolds, P. A. Henkart, *Proc. Natl. Acad. Sci. U.S.A.* **81**, 5551 (1984).
10. E. R. Podack and P. J. Konigsberg, *J. Exp. Med.* **160**, 695 (1984).
11. J. D.-E Young, C. F. Nathan, Z. A. Cohn, *J. Cell. Biochem. Suppl.* **9A**, 161 (1985); J. D.-E Young, C. F. Nathan, E. R. Podack, M. A. Palladino, Z. A. Cohn, *Proc. Natl. Acad. Sci. U.S.A.* **83**, 150 (1986).
12. D. Masson, P. Corthesy, M. Nabholz, J. Tschopp, *EMBO J.* **4**, 2533 (1985).
13. M. Criado, J. M. Lindstrom, C. G. Anderson, G. Dennert, *J. Immunol.* **135**, 4245 (1985).
14. J. H. Humphrey and R. R. Dourmashkin, *Adv. Immunol.* **11**, 75 (1969).
15. S. Bhakdi, O. J. Bjerrum, U. Rother, H. Knufermann, D. F. H. Wallach, *Biochim. Biophys. Acta* **406**, 21 (1975); S. Bhakdi and J. Tranum-Jensen, *ibid.* **737**, 343 (1983).
16. G. Biesecker, E. R. Podack, C. A. Halverson, H. J. Müller-Eberhard, *J. Exp. Med.* **149**, 448 (1979).
17. M. M. Mayer, *Proc. Natl. Acad. Sci. U.S.A.* **69**, 2954 (1972); M. M. Mayer, D. W. Michaels, L. E. Ramm, M. B. Whitlow, J. B. Willoughby, M. L. Shin, *CRC Crit. Rev. Immunol.* **2**, 133 (1981).
18. R. R. Dourmashkin, *Immunology* **35**, 205 (1978).
19. E. R. Podack and J. Tschopp, *Proc. Natl. Acad. Sci. U.S.A.* **79**, 574 (1982); E. R. Podack and J. Tschopp, *J. Biol. Chem.* **257**, 15204 (1982).
20. J. Tschopp, H. J. Müller-Eberhard, E. R. Podack, *Nature (London)* **298**, 534 (1982).
21. K. Yamamoto and M. Takahashi, *Int. Arch. Allergy Appl. Immunol.* **48**, 653 (1975).
22. J. Tschopp, *Fed. Proc. Fed. Am. Soc. Exp. Biol.* **43**, 1450 (1984).
23. M. Montal and P. Mueller, *Proc. Natl. Acad. Sci. U.S.A.* **69**, 3561 (1972).
24. If we assume that the pore to be formed is a cylindrical structure filled with an aqueous solution of the same specific conductance as the external solution, we can estimate the size of the pore from the magnitude of each discrete conductance (g_o) step by the relation $g_o = \sigma\pi r^2/l$, in which σ is the specific conductance of the aqueous phase and r and l are the radius and length of the pore, respectively [R. Benz, K. Janko, W. Boos, P. Lauger, *Biochim. Biophys. Acta* **511**, 305 (1978)]. For an average tubular length of 160 Å (*19*) and conductance of 1.5 nS (0.1*M* NaCl) (Fig. 5D), the estimated diameter is 60 Å. Boiling in SDS increases the tubular length to 200 to 220 Å (*19*). With a mean conductance of 2 nS (Fig. 5E), the estimated diameter is 80 Å. Although this kind of estimate has been shown to hold for large pores of the type described here, inference of channel size from single channel conductance should be viewed with caution as the two may not always correlate [B. L. Kagan, A. Finkelstein, M. Colombini, *Proc. Natl. Acad. Sci. U.S.A.* **78**, 4950 (1981)].
25. E. B. Giavedoni, Y. M. Chow, A. P. Dalmasso, *J. Immunol.* **122**, 240 (1979).
26. L. E. Ramm and M. M. Mayer, *ibid.* **124**, 2281 (1980).
27. The ion selectivity was determined from the reversal potential necessary to null current flow from a tenfold higher salt concentration, with the *cis* (positive) compartment being more concentrated. The reversal potential was converted into selectivity ratios with the use of the Nernst-Planck equation. Experiments with MAC were performed with purified C5b-6, C7, C8, and C9 (*19, 20*), added in the sequence C5b-6, C8, C7, and C9 at molar ratios of 1:1:1:12, respectively. The ion selectivity experiments with MAC were performed as before.
28. Permeability increase to ^{14}C-labeled sucrose was assessed by a filtration assay [J. D.-E Young, J. C. Unkeless, H. R. Kaback, Z. A. Cohn, *Proc. Natl. Acad. Sci. U.S.A.* **80**, 1636 (1983)]. Poly C9 vesicles were formed (Fig. 1) and equilibrated

in ^{14}C-labeled sucrose. The reaction was initiated by diluting the vesicle preparation into an equiosmolar solution of sodium isothionate, and at intervals samples of the reaction mixture were filtered and washed; the radioactive material remaining on the filter was then determined. Membrane permeability increase to Lucifer yellow was assessed by diluting poly C9 vesicles containing Lucifer yellow 1:10 with equiosmolar buffer, followed by sedimentation and washing twice of the vesicles by high-speed centrifugation. The amount of Lucifer yellow trapped in the vesicles was determined by fluorescence (excitation, 430 nm; emission, 540 nm). Control vesicles under similar conditions trapped most of the input of Lucifer yellow.

29. Several monospecific polyclonal antisera to C9 and perforin were prepared in rabbits as follows. Immunization was always done through multiple sites with 50 to 125 μg of C9 or 10 to 30 μg of perforin resuspended in complete Freund's adjuvant. Antigens used for boosts were resuspended in incomplete adjuvant to 10 to 50 μg per rabbit. The rabbits were given booster injections of antigen 2 to 3 weeks after primary immunization at 1- to 2-week intervals and blood was withdrawn 3 to 7 days after the booster. The following antisera were obtained: (i) antisera to reduced and alkylated C9, and glutaraldehyde-linked C9; (ii) antisera to native C9 and C9 boiled in 1 percent SDS; (iii) antisera to native perforin purified by means of a Mono Q column procedure (*7, 8*); (iv) antisera to reduced and alkylated perforin. Reduction and alkylation were performed with 20 m*M* DTT for 2 hours at 37°C, followed by 50 m*M* iodoacetamide for 1 hour at room temperature in the dark. Glutaraldehyde-treated samples were adjusted to final 0.05 to 0.1 percent glutaraldehyde. For immunoblots, antisera were used at 1:50 dilutions. Immunoblots were performed according to H. Towbin, T. Staehelin, J. Gordon [*Proc. Natl. Acad. Sci. U.S.A.* 76, 4350 (1979)] with goat antiserum to rabbit immunoglobulin G (IgG)–peroxidase (Bio-Rad) or ^{125}I-labeled protein A (ICN) as the second specific binding reagent.
30. The IgG fraction was obtained from the native perforin antiserum (*29*) by ammonium sulfate precipitation, with ammonium sulfate adjusted to 45 percent by volume, and subsequent elution through DEAE Affigel Blue column (Bio-Rad) with a linear NaCl gradient. The eluted IgG was dialyzed against 0.1*M* sodium acetate buffer, *p*H 5.5, concentrated to 5 mg/ml in sodium acetate buffer containing 2 m*M* EDTA, 10 m*M* β-mercaptoethanol, and 3 m*M* NaN_3, and subjected to papain digestion (papain at 1:100, by weight) for 16 hours at 37°C. The Fab fraction was purified with DEAE Affigel column and dialyzed against 0.2*M* sodium borate buffer, *p*H 8.3, containing 0.5*M* NaCl, and coupled to CNBr-activated Sepharose 4B essentially as described by S. C. March, I. Parikh, and P. Cuatrecasas [*Anal. Biochem.* **60**, 149 (1974)]. The coupling efficiency was approximately 1.1 mg of protein per milliliter of Sepharose. For purification of perforin, cytotoxic T cell granules [isolated from CTLL-R8 and CTLL-A11 (*7, 8*)] were extracted with 0.5*M* $NaKHPO_4$ buffer, *p*H 7.4, containing 1 m*M* EDTA, 10 m*M* benzamidine, and 3 m*M* NaN_3, as described (*7*). The clear high-speed centrifugation supernatant (*7*) was adjusted with 0.5 percent deoxycholate and batch-adsorbed with antibody to perforin Fab-Sepharose (at 1 mg of Fab per 1 mg of granule protein) for 2 hours at 4°C with continuous agitation, followed by three 5-minute washings with the same buffer. The immunoadsorbent was packed into a small syringe, equilibrated with 0.5 percent deoxycholate in TBS. The antigen was eluted with 0.1*M* triethylamine, *p*H 11; it was immediately neutralized by collection of eluate in tubes containing 1 *M* tris-HCl, *p*H 7.4 at 20 percent of the column volume [I. S. Mellman and J. C. Unkeless, *J. Exp. Med.* **152**, 1048 (1980)]. The antigen was also eluted with 0.2*M* glycine-HCl, *p*H 2.5. This material was tested directly for hemolysis and for functional channel formation in the planar bilayer.
31. The isolated perforin from lymphocytes inserts spontaneously into planar bilayers in the presence of calcium and at room temperature (22° to 24°C) to form ion channels with a minimal unit conductance of 0.4 nS in 0.1*M* NaCl. As described (*8, 11*), perforin that has been polymerized in lipid vesicles at 37°C produces larger unit conductances, ranging from 1 to 6 nS in 0.1*M* NaCl. These observations suggest that perforin may form functional channels before becoming fully polymerized as tubular lesions.
32. P. Barfort, E. R. Arquilla, P. O. Vogelhut, *Science* **160**, 1119 (1968); D. Wobschall and C. McKeon, *Biochim. Biophys. Acta* **413**, 317 (1975).
33. D. W. Michaels, A. S. Abramovitz, C. H. Hammer, M. M. Mayer, *Proc. Natl. Acad. Sci. U.S.A.* **73**, 2852 (1976).
34. M. B. Jackson, C. L. Stephens, H. Lecar, *Proc. Natl. Acad. Sci. U.S.A.* **78**, 6421 (1981). The channels observed by this group have smaller unit conductances (90 pS in 0.15*M* NaCl) and much shorter open channel lifetimes than the poly C9 channels observed here. Similar kinetics and channel sizes were observed with C5b-C8 incorporated into planar bilayers and patch clamped membranes. Since whole serum was used by Jackson *et al.* as a source of complement, it is possible that the channels observed by that group reflected only the insertion of C5b-C8 channels. Our attempts to study insertion of C9 into patch-clamped membranes by the sequential addition of defined C components (C5b-C9) invariably resulted in rapid loss of the gigaohm seal only upon addition of C9.
35. U. Hadding and H. J. Müller-Eberhard, *Immunology* **16**, 719 (1969).
36. These data were obtained with C9 incorporated into lipid, and with lipid in excess amount. The C9-lipid mixture was then transferred to the planar bilayer. Channels with small unit conductances (0.2 to 0.4 nS in 0.1*M* NaCl) were selected by this procedure. Examination of this specimen by electron microscopy failed to reveal the typical ringlike lesions. These observations are in accord with recently published results that have argued for membrane damage and channel formation prior to complete polymerization of C9 or MAC into the supramolecular tubular complexes [J. R. Dankert and A. F. Esser, *Proc. Natl. Acad. Sci. U.S.A.* **82**, 2128 (1985); S. Bhakdi and J. Tranum-Jensen, *J. Immunol.* **136**, 2999 (1986)].
37. J. D.-E Young, J. C. Unkeless, T. M. Young, A. Mauro, Z. A. Cohn, *Nature (London)* **306**, 186 (1983); J. D.-E Young, M. Blake, A. Mauro, Z. A. Cohn, *Proc. Natl. Acad. Sci. U.S.A.* **80**, 3831 (1983).
38. Poly C9 can be formed from monomeric C9 after its incubation with Zn^{2+} at 37°C in either the presence or absence of lipid vesicles and detergent. Poly C9 in solution remains soluble but requires detergent for incorporation into bilayers. Thus, any reagent that polymerizes C9 in solution should also abolish its membrane insertion capability, rendering C9 inactive. This observation should explain why Zn^{2+} inactivates the C9-dependent hemolytic activity of human serum (*21*). For the planar bilayer experiments described here, both poly C9 formed in solution, without lipid or detergent, and that formed in lipid vesicles were used (Figs. 3 and 4). A homogeneous population of circular polymers can be obtained by boiling poly C9 in SDS and deoxycholate followed by rate zonal centrifugation (legend to Fig. 1G). This homogeneous material was used here for single channel studies (Fig. 5).
39. J. Zimmerberg, F. S. Cohen, A. Finkelstein, *Science* **210**, 906 (1980); F. S. Cohen, M. H. Akabas, J. Zimmerberg, A. Finkelstein, *J. Cell Biol.* **98**, 1054 (1984); T. M. Young and J. D.-E Young, *Biochim. Biophys. Acta* 775, 441 (1984).
40. We thank S. S. Ko and M. A. DiNome for technical assistance. Supported by a Cancer Research Institute and a Lucille P. Markey Charitable Trust grant to J.D.-EY.; by grants CA30198 and AI070127 from NIH to Z.A.C.; and by NIH grants AI18525 and CA34524 and by the American Cancer Society grant IM396 to E.R.P. J.D.-EY. is a Lucille P. Markey Scholar. E.R.P. is an established investigator of the American Heart Association.

31 January 1986; accepted 4 June 1986